INTERNATIONAL JOURNAL FOR NUMERICAL METHODS IN FLUIDS, VOL. 17, 291–300 (1993)

LINEAR STABILITY OF SWIRLING FLOWS COMPUTED AS SOLUTIONS TO THE QUASI-CYLINDRICAL EQUATIONS OF MOTION

ROBERT E. SPALL

Dept of Mechanical Engineering, University of South Alabama, EGCB 212, Mobile, AL 36688, U.S.A.

SUMMARY

The linear stability of numerical solutions to the quasi-cylindrical equations of motion for swirling flows is investigated. Initial conditions are derived from Batchelor's similarity solution for a trailing line vortex. The stability calculations are performed using a second-order-accurate finite-difference scheme on a staggered grid, with the accuracy of the computed eigenvalues enhanced through Richardson extrapolation. The streamwise development of both viscous and inviscid instability modes is presented. The possible relationship to vortex breakdown is discussed.

KEY WORDS Vortex breakdown Linear stability Swirling flows

1. INTRODUCTION

Over the past 30 years, considerable effort has been expended toward an understanding of the mechanisms inherent in the development and evolution of longitudinal vortices. This has been motivated, in part, by the desire to control and/or disable these vortices in applications such as the aircraft-wake–vortex hazard and submarine non-acoustic stealth. Methods which have been suggested to reduce the intensity of these vortices, and have received considerable attention are: (1) to excite vortex instabilities, and (2) to promote vortex bursting or breakdown.

The present paper addresses primarily the first mechanism; that is, viscous and inviscid instability of a prototype trailing line vortex. Previous viscous stability calculations of the 'q-vortex' (derived from the far-wake solution for a trailing line vortex[1] have been performed by Lessen and Paillet,[2] Stewartson[3] and Khorrami.[4] Several other researchers have investigated the inviscid stability of these profiles (cf. References 5–9). Results show that the stability of the vortex is strongly dependent on the value of q (related to the ratio of the maximum swirl velocity to the maximum axial velocity). The vortex is completely stabilized for values of $q > 1{\cdot}5$, with the most unstable wave obtained in the limit $|n| \to \infty$ (where n is the azimuthal wavenumber). Certain restrictions are inherent when employing Batchelor's solution for stability calculations. Batchelor's solution depends on a partial linearization of the quasi-cylindrical equations of motion. Requirements for this linearization are: (1) the circumferential velocity is small compared to the free-stream axial velocity; and (2) the axial velocity within the vortex core is nearly equal to the free-stream velocity. Hall[10] provides comparisons between the similarity solutions and the numerical solutions to the quasi-cylindrical equations of motion at swirl ratios comparable to those considered in this paper. His conclusion was that, as the vortex evolves in space, Batchelor's solution provides a poor fit to the numerically determined axial velocity profile and a good fit to

0271–2091/93/160291–10$10.00

Received 27 April 1992
Revised 1 March 1993

the circumferential velocity profile (although, even here, differing somewhat)—the only contribution to this discrepancy being the linearization process.

The q-vortex has also been fit to vortices formed within tube-and-vane type apparatus—often as a means of studying vortex breakdown. Experiments reveal that profiles slightly upstream of breakdown have values of $q > 1{\cdot}5$, which indicates that these vortices are stable to both symmetric and asymmetric inviscid disturbances (cf. References 11 and 12). It is known that numerical solutions of quasi-cylindrical equations fail under certain conditions; that is, when the ratio of the maximum swirl velocity to axial velocity exceeds (approximately) unity (cf. Reference 13). It has then been proposed that this point may correspond to the approximate location of the onset of vortex breakdown. It is of interest to investigate the stability of profiles of this type. This may shed additional light on the possible role of flowfield instabilities in determining the resultant form of vortex breakdown. Of course, the symmetry assumption prevents one from correlating the form of an impending breakdown. To overcome such restrictions, solutions to the fully three-dimensional Navier–Stokes equations for vortex breakdown (cf. Reference 14) need be investigated—certainly a more difficult task.

The stability calculations are performed using a normal mode analysis. Although, strictly speaking, a non-parallel stability theory is appropriate (multiple scales[15] or parabolized stability equation approach[16]), the quasi-parallel flow assumption is made. The quasi-parallel assumption is justified on the grounds that the vortex is embedded in a zero pressure gradient flow and that velocity changes along the vortex axis (upstream from any impending breakdown), due only to viscous forces, are small. At high Reynolds numbers, significant changes occur over many wavelengths. Of course, for a swirling flow the pressure is not constant across the core, but varies according to the square of the circulation. Thus, an adverse pressure gradient may exist along the axis for a vortex embedded in a zero pressure gradient free stream. It is also noted that the quasi-parallel assumption has proven invaluable in providing an insight into the stability of laminar boundary layers. Provisions are made to include some non-parallel effects by retaining radial velocity and streamwise derivative terms in the mean flow (absent in studies of the q-vortex). The stability formulation is based on second-order-accurate finite-difference approximations on a staggered grid, with the accuracy of the computed eigenvalues being improved through Richardson extrapolation.

2. PROBLEM FORMULATION

2.1. *Mean flow*

The linear stability of solutions to the quasi-cylindrical equations of motion is considered. The quasi-cylindrical equations are derived from the laminar, incompressible, axisymmetric equations of motion as a result of boundary-layer type assumptions; that is, axial gradients are small compared to radial gradients (cf. Reference 13). The problem is parabolic in the streamwise direction and thus the equations may be solved by marching in z. The quasi-cylindrical equations were first solved by Hall[10] using finite-difference methods for several sets of initial and boundary conditions.

The objective of the present study is to investigate the linear stability of a longitudinal vortex embedded in a zero pressure gradient free stream. To this end, initial conditions are derived from the far-wake similarity solution to the trailing line vortex.[1] The circumferential and axial velocity profiles, respectively, are given as

$$v^* = \frac{\lambda}{r^*}(1 - e^{-ar^{*2}}); \tag{1}$$

$$w^* = W_\infty + W_0 e^{-ar^{*2}}, \tag{2}$$

where λ and a are constants, and W_0 represents the centreline axial velocity.

As previously mentioned, the q-vortex has been employed in many previous stability studies. In the present study, the length scale (l) is chosen as the vortex core radius (the radius at which the swirl velocity is a maximum), and thus $l = 1{\cdot}122/\sqrt{a}$. The velocity scale is chosen as the far-field axial velocity, W_∞. The non-dimensional forms of (1) and (2) become

$$v = \frac{\hat{q}}{r}(1 - e^{-(1{\cdot}122r)^2}), \tag{3}$$

$$w = 1 + \delta e^{-(1{\cdot}122r)^2}, \tag{4}$$

where $\hat{q} = \sqrt{a\lambda}/1{\cdot}122\ W_\infty$ and $\delta = W_0/W_\infty$.

Due to different scaling parameters, the definitions of $\hat{q}$ and δ here differ from those defined in previous studies of the q-vortex (cf. Reference 5). The radial boundary conditions are specified as $w = 1$ and $v = v(r_0)$, where r_0 represents the edge of the computational domain. The above equations are solved using standard second-order-accurate finite-difference approximations, marching in the streamwise direction. Grid resolutions used in the solution procedure were sufficient to ensure that the stability characteristics of the mean flow profiles are grid-independent.

2.2. *Stability equations*

Briefly, the stability equations are derived by first linearizing the equations of motion and then expressing the linearized perturbation variables in the form

$$\{u', v', w', p'\} = \{iF(r), G(r), H(r), P(r)\}e^{i(\alpha z + n\theta - \omega t)}. \tag{5}$$

Here α is the real axial wavenumber, n is the real azimuthal wavenumber, and ω is complex (thus, we are considering temporal stability). These equations, consisting of three second-order momentum equations and the continuity equation, have previously been given in Reference 2 and may be expressed in the form

$$(A\mathrm{D}^2 + B\mathrm{D} + C)\,\bar{\Phi} = 0, \tag{6}$$

where $\bar{\Phi}$ is a four-element vector defined by $\bar{\Phi} = \{F, G, H, P\}^t$. $\mathrm{D} \equiv \partial/\partial r$, where r is the radial co-ordinate. The non-zero coefficients of 4×4 matrices A, B and C are given in the Appendix. The above equations are solved subject to the following boundary conditions (see Reference 17):

at $r = 0$,

$$\text{if } n = 0, \quad \Phi_1(0) = \Phi_2(0) = 0, \qquad \Phi_3'(0) = 0, \tag{7}$$

$$\text{if } n = \pm 1, \quad \Phi_1(0) \pm \Phi_2(0) = 0, \qquad \Phi_1'(0) = 0, \qquad \Phi_3(0) = 0, \tag{8}$$

$$\text{if } |n| > 1, \quad \Phi_1(0) = \Phi_2(0) = \Phi_3(0) = 0, \tag{9}$$

as $r \to \infty$,

$$\Phi_1 = \Phi_2 = \Phi_3 = 0. \tag{10}$$

The solution technique employed is based on a second-order-accurate finite-difference approximation on a staggered mesh. The staggered mesh eliminates the need for pressure boundary conditions. The scheme is analagous to that employed quite successfully in the compressible boundary-layer stability code COSAL.[18,19] A brief description follows.

The radial co-ordinate, r, is first mapped onto a computational domain $0 \leqslant \eta \leqslant 1$ using the mapping

$$\eta = 1 - \frac{\ln\{[\beta + 1 - (r/r_0)]/[\beta - 1 + (r/r_0)]\}}{\ln[(\beta+1)/(\beta-1)]}, \tag{11}$$

where $1 < \beta < \infty$. As $\beta \to 1$, more points are clustered toward the vortex centreline.

The second-order-accurate finite-difference representation of the stability equations is then given as

$$\frac{A_j \eta_r^2}{\Delta\eta^2}(\bar{\Phi}_{j+1} - 2\bar{\Phi}_j + \bar{\Phi}_{j-1}) + d_1\left\{\frac{A_j\eta_{rr} + B_j\eta_r}{2\Delta\eta}(\bar{\Phi}_{j+1} - \bar{\Phi}_{j-1}) + C_j\bar{\Phi}_j\right\}$$
$$+ d_2\left\{\frac{C_j}{2}(\bar{\Phi}_{j+1/2} + \bar{\Phi}_{j-1/2}) + \frac{B_j\eta_r}{\Delta\eta}(\bar{\Phi}_{j+1/2} - \bar{\Phi}_{j-1/2})\right\} \qquad (j = 1, 2, \ldots, N-1) \tag{12}$$

where $\bar{\Phi}$ has components $\Phi_{k,j}$ $(k = 1, \ldots, 4)$ and $j = 0$ at the vortex centreline and $j = N$ at the radial boundary. In addition, $d_1 = 1$, $d_2 = 0$ for F, G, and H components of $\bar{\Phi}$; $d_1 = 0$, $d_2 = 1$ for the P component.

The first-order continuity equation is represented as

$$\left[B_{j+1/2}\frac{\eta_r}{\Delta\eta} + \frac{C_{j+1/2}}{2}\right]\bar{\Phi}_{j+1} + \left[\frac{C_{j+1/2}}{2} - B_{j+1/2}\frac{\eta_r}{\Delta\eta}\right]\bar{\Phi}_j + \gamma\omega\bar{\Phi}_{j+1/2} = 0 \quad (j = 0, 1, \ldots, N-1). \tag{13}$$

The term $\gamma\omega\bar{\Phi}_{j+1/2}$, denoting an artificial compressibility factor,[20] is added to the continuity equation to make the coefficient matrix non-singular. When γ is assigned a value of order 10^{-10}, the compressibility factor has no effect on the desired eigenvalues. The above equations, along with six boundary conditions, represent $4N+3$ equations for $4N+3$ unknowns. This system constitutes a generalized eigenvalue problem of the form

$$\hat{A}\bar{\Phi} = \hat{B}\omega\bar{\Phi}, \tag{14}$$

which is solved for the eigenvalues ω using the IMSL QL routine CXLZ. The accuracy of the desired eigenvalue is improved by Richardson extrapolation.[21]

3. RESULTS

The linear stability of solutions to the quasi-cylindrical equations are computed for both high and low swirl ratio cases. As a prelude to this presentation, it is noted that results were computed for a viscous mode of the q-vortex which has previously been published in the literature.[4] The main purpose of this was to verify the accuracy of the solution procedure. The mean flow profiles were given in analytic form as $V = q/r(1 - e^{-r^2})$, $W = W_\infty/W_0 + e^{-r^2}$, $U = 0$, where $W_\infty/W_0 = 1$ and $q = 0{\cdot}4$. In addition, the Reynolds number was taken as 2000 (based on scalings in Reference 4). The results of the finite-difference scheme agreed to eight decimals with the spectral scheme when a maximum of 120 points were used. This accuracy is clearly sufficient for the purposes of the present analysis. Thus, this resolution was used for the results presented in the remainder of the paper. (For preliminary searches, 60 points with no extrapolation was found to be sufficient.)

Mean flows were computed as solutions to the quasi-cylindrical equations of motion. In the solution of these equations, 400 points were used in the radial direction, with a stretching function [equation (11)] employed to cluster points near the vortex core. The far-field boundary was set to

$r_0 = 40$ (i.e. 40 core radii as defined at the inflow plane). The radius was chosen large enough so that the zero perturbation radial boundary conditions required for the stability equations would be satisfied. A rather large number of points in the radial direction was necessary in order to provide sufficiently accurate radial derivative terms.

The calculations were performed for both low and high swirl ratio cases. As expected, the low swirl ratio case ($\hat{q} = 0{\cdot}4$, $\delta = 1{\cdot}0$) provided stability results in good agreement with previous results appearing in the literature for both viscous and inviscid modes of the prototype q-vortex. The inclusion of the non-parallel terms in the stability analysis had only a mild destabilizing effect. Thus, these results are not discussed further.

Conditions for the high swirl case were chosen in the range where vortex breakdown may be expected to occur. Specifically, $\hat{q} = 1{\cdot}75$ and $\delta = 1{\cdot}0$. The Reynolds number at inflow was taken as 1000. The swirl and axial velocity profiles are shown in Figures 1(a) and 1(b), respectively, at axial locations $z = 0$, 30, 60 and 90. The numerical solution of quasi-cylindrical equations failed at $z = 98{\cdot}75$. (The numerical procedure fails to converge, as first described by Hall.[13]) Note that at $z = 90$, the centreline axial velocity has dropped below the free-stream axial velocity, while at the core edge ($r \approx 1{\cdot}5$) the axial velocity exceeds the free-stream axial velocity. Thus, two inflection points exist in this profile. Shown in Figure 1(c) are the maximum swirl velocity, centreline axial velocity and pressure, and swirl ratio as a function of axial distance. The most important difference between these results and those for the low swirl case concern the behaviour of the swirl ratio. Here the swirl ratio increases in the streamwise direction, from $\approx 0{\cdot}63$ at inflow to $\approx 1{\cdot}1$ at $z = 98$, the point at which the solution procedure fails. Clearly, the assumptions used in the derivation of Batchelor's solution are violated under these conditions. Although not shown, the swirl ratio decreases continuously for the low swirl case. Note that the increase is approximately linear for $z < 75$, and beyond this region begins to increase in an exponential manner. At failure, the swirl ratio is certainly in the range at which vortex breakdown is expected to occur. Thus, it is reasonable to assume that these profiles are characteristic of those leading to vortex breakdown. Of course, the form of vortex breakdown cannot be predicted due to the assumption of symmetry.

The stability results are presented next. Growth rate results are presented in Figure 2(a) for the viscous axisymmetric ($n = 0$) mode at axial locations $z = 0$, 30, 60 and 90. The calculations shown in this figure include non-parallel mean flow terms. When the non-parallel effects are neglected, the modes shown in the figure exist, but are stable. As the figure indicates, the growth rates for $0 \leqslant z \leqslant 60$ remain nearly constant, but at $z = 90$ have increased by a factor of 2. The maximum growth rates occur for low values of wavenumber, indicating that these are long-wavelength instabilities. The results for $n = 1$ mode are shown in Figure 2(b), which again include non-parallel effects. Here the increase in growth rates at $z = 90$ occurs, although the increase is not so dramatic as it was for the $n = 0$ mode. Also, the maximum growth rates occur for infinite wavelength disturbances ($\alpha = 0$, where, strictly speaking, the quasi-parallel flow assumption is inapplicable, although may provide reasonable results).

The results for the $n = -1$ inviscid mode are shown in Figure 2(c). Here the instability appears only after the vortex has evolved some distance in the streamwise direction. The amplitude of the instability at $z = 90$ is comparable to the amplitude of the viscous modes at the same location. Again, the mode was stable when U and $\partial W/\partial z$ were set to zero. Thus, these non-zero components of the mean flow, which are driven by the interaction between the swirl and axial velocity, appear to become important at high swirl rates.

It is proposed that the above disturbance modes may have an effect on the resultant form of vortex breakdown. That is, although they do not provide a mechanism for the initiation of breakdown, they may have an effect on the breakdown structure itself. Of course, confirmation of instability at these swirl levels must await a fully non-parallel stability formulation.

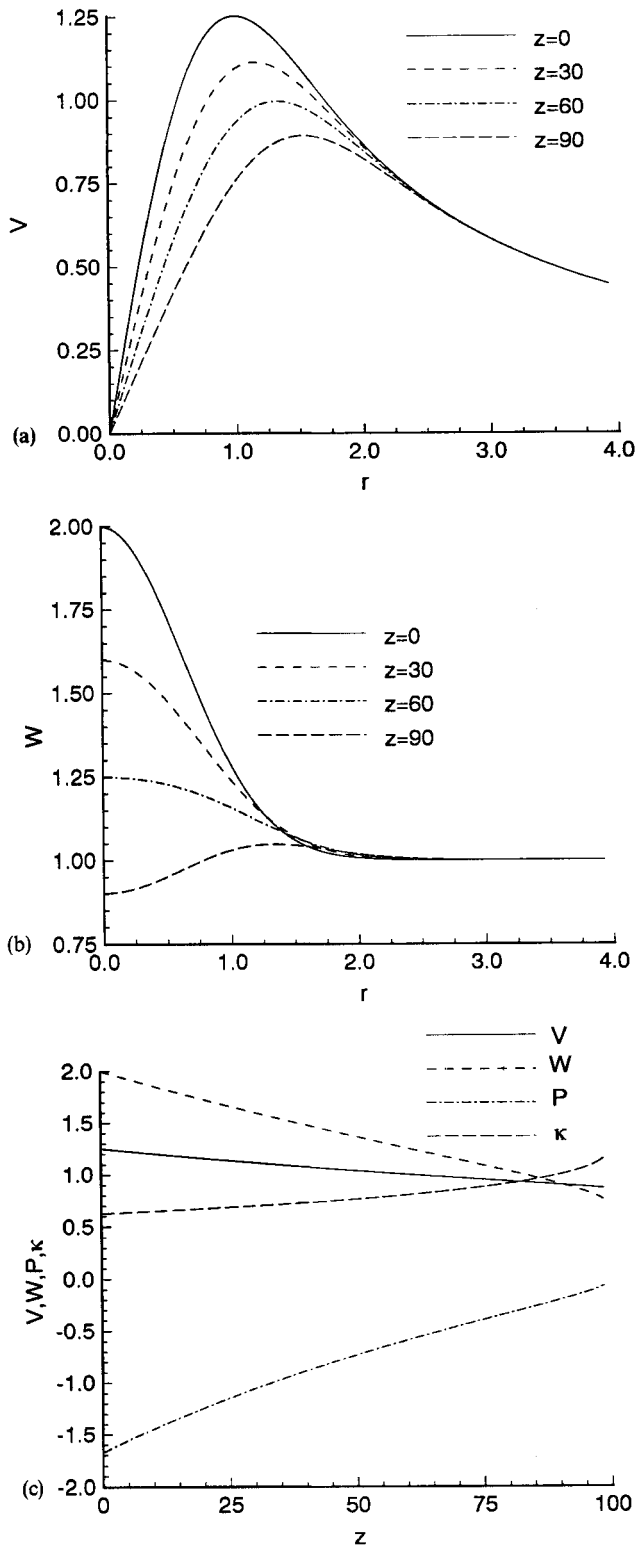

Figure 1. Meanflow solutions for high swirl case; $\hat{q}=1{\cdot}75$, $\delta=1{\cdot}0$, $Re_i=1000$: (a) swirl velocity profiles; (b) axial velocity profiles; (c) streamwise variations of V. W, P and κ.

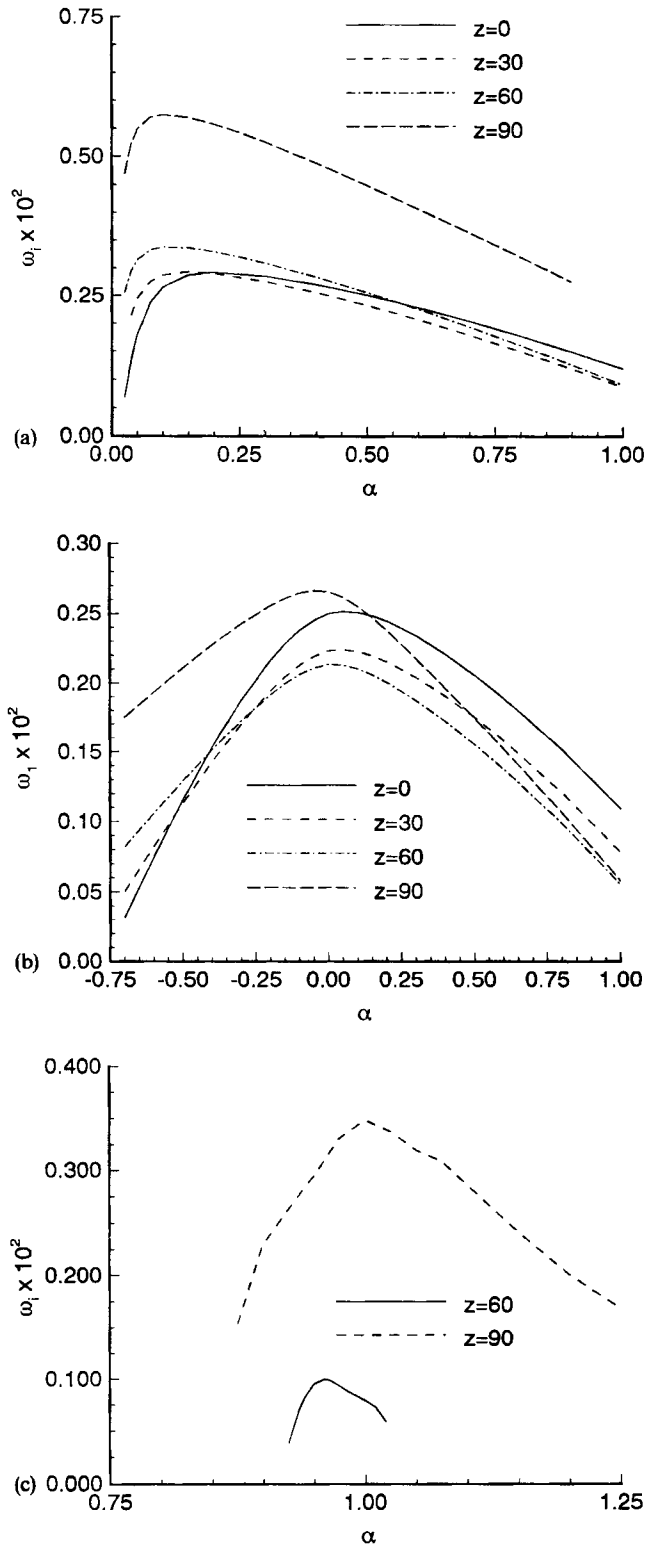

Figure 2. Growth rates at several axial locations: (a) viscous mode, $n=0$; (b) viscous mode $n=1$; (c) inviscid mode, $n=-1$.

4. CONCLUSIONS

The linear stability of a quasi-cylindrical vortex evolving in the streamwise direction was investigated. The vortex was embedded in a uniform free stream, and thus evolved due to viscous effects alone. The mean flow profiles were computed as numerical solutions to the quasi-cylindrical equations of motion. The advantage of this procedure rests in its generality. That is, the requirements necessary for partial linearization of the quasi-cylindrical equations, as predicted in Batchelor's solution (from which the q-vortex is derived), may be relaxed. The stability results for the low swirl case were consistent with those found by others for analytic profiles given by the q-vortex, although this was not known *a priori*. For the high swirl case, no instability was detected when non-parallel terms in the mean flow profiles were absent. Based on previous studies of the q-vortex, this result was not unexpected (cf. Reference 12). When the non-parallel terms were included, viscous and inviscid instability was noted. The magnitude of the instability increased as the location of the point of failure of the numerical solution to the quasi-cylindrical equations was approached (to within ≈ 9 core radii). This may have implications in important areas such as vortex breakdown. Of course, at this location, the quasi-parallel flow approximation is suspect, and confirmation awaits results from a fully non-parallel formulation.

Further work into the stability of these swirling flows is anticipated by the author. To fully account for non-parallel effects, a multiple-scale technique will be attempted. The stability of solutions to the quasi-cylindrical equations with imposed external pressure gradients will also be investigated.

ACKNOWLEDGEMENTS

The author acknowledges the Alabama Supercomputer Authority and the Theoretical Flow Physics Branch at NASA Langley Research Center for providing the necessary computational resources.

APPENDIX

The non-zero components of the 4×4 matrices A, B, C are given as

$$A(1,1) = -\frac{\mathrm{i}}{Re},$$

$$A(2,2) = -\frac{1}{Re},$$

$$A(3,3) = -\frac{1}{Re},$$

$$B(1,1) = \mathrm{i}\left[U - \frac{1}{Re\, r}\right],$$

$$B(1,4) = 1,$$

$$B(2,2) = U - \frac{1}{Re\, r},$$

$$B(3,3) = U - \frac{1}{Re\, r},$$

$$B(4,1)=1,$$

$$C(1,1)=\omega+\mathrm{i}\frac{\mathrm{d}U}{\mathrm{d}r}-\frac{nV}{r}-\alpha W+\frac{i}{Re}\left(\frac{n^2+1}{r^2}+\alpha^2\right),$$

$$C(1,2)=\frac{\mathrm{i}2n}{Re\,r^2}-\frac{2V}{r},$$

$$C(2,1)=\mathrm{i}\frac{\mathrm{d}V}{\mathrm{d}r}+\frac{2n}{Re\,r^2}+\frac{\mathrm{i}V}{r},$$

$$C(2,2)=-\mathrm{i}\omega+\frac{\mathrm{i}nV}{r}+\mathrm{i}\alpha W+\frac{U}{r}+\frac{1}{Re}\left(\frac{n^2+1}{r^2}+\alpha^2\right),$$

$$C(2,4)=\frac{\mathrm{i}n}{r},$$

$$C(3,1)=\mathrm{i}\frac{\mathrm{d}W}{\mathrm{d}r},$$

$$C(3,3)=-\mathrm{i}\omega+\frac{\mathrm{i}nV}{r}+\mathrm{i}\alpha W+\frac{\mathrm{d}W}{\mathrm{d}z}+\frac{1}{Re}\left(\frac{n^2}{r^2}+\alpha^2\right),$$

$$C(3,4)=\mathrm{i}\alpha$$

$$C(4,1)=\frac{1}{r},$$

$$C(4,2)=\frac{n}{r},$$

$$C(4,3)=\alpha.$$

REFERENCES

1. G. K. Batchelor, 'Axial flow in trailing line vortices', *J. Fluid Mech.*, **20,** 645–658 (1964).
2. M. Lessen and F. Paillet, 'The stability of a trailing line vortex. Part 2. Viscous theory', *J. Fluid Mech.*, **65,** 769–779 (1974).
3. K. Stewartson, 'The stability of swirling flows at large Reynolds numbers when subjected to disturbances at large azimuthal wavenumber', *Phys. Fluids*, **25,** 1953–1957 (1982).
4. M. Khorrami, 'On the viscous modes of instability of a trailing line vortex', *J. Fluid Mech.*, **225,** 197–212 (1991).
5. M. Lessen, P. J. Singh and F. Paillet, 'The stability of a trailing line vortex. Part 1. Inviscid theory', *J. Fluid Mech.*, **63,** 753–763 (1974).
6. P. W. Duck and M. R. Foster, 'The inviscid stability of trailing line vortex', *Z. Angew. Math. Phys.*, **31,** 523–530 (1980).
7. S. Leibovich and K. Stewartson, 'A sufficient condition for the instability of columnar vortices', *J. Fluid Mech.*, **126,** 335–356 (1983).
8. K. Stewartson and K. Capell, 'On the stability of ring modes in a trailing line vortex: the upper neutral points', *J. Fluid Mech.*, **156,** 369–386 (1985).
9. P. Duck, 'The inviscid stability of swirling flows: large wavenumber disturbances', *Z. angew. Math. Phys.*, **37,** 340–360 (1986).
10. M. G. Hall, 'A numerical method for solving the equations for a vortex core', *Royal Aircraft Establishment Tech. Rep. No. 65106*, May 1965.
11. A. K. Garg, 'Oscillatory behavior in vortex breakdown flows: an experimental study using a laser doppler anemometer', *M.S. Thesis*, Cornell University, Ithaca, NY.
12. S. Leibovich, 'The structure of vortex breakdown', *Ann. Rev. Fluid Mech.*, **10,** 221–246 (1978).
13. M. G. Hall, 'Vortex breakdown', *Ann. Rev. Fluid Mech.*, **4,** 195–218 (1972).
14. R. E. Spall and T. B. Gatski, 'A computational study of the topology of vortex breakdown', *Proc. Roy. Soc. Lond. A*, **435,** 321–337 (1991).

15. W. S. Saric and A. H. Nayfey, 'Nonparallel stability of boundary-layer flows', *Phys. Fluids*, **8,** 945–950 (1975).
16. F. P. Bertolotti, 'Compressible boundary layer stability analyzed with the PSE equations', *AIAA-91-1637*, AIAA 22nd Fluid Dynamics, Plasma Dynamics & Lasers Conference, Honolulu, Hawaii, June 1991,
17. G. K. Batchelor and A. E. Gill, 'Analysis of the stability of axisymmetric jets', *J. Fluid Mech.*, **14,** 529–551 (1962).
18. M. R. Malik and S. A. Orszag, 'Efficient computation of the stability of three-dimensional compressible boundary layers', *AIAA-81-1277*, AIAA 14th Fluid and Plasma Dynamics Conference, Palo Alto, CA, June 1981.
19. M. R. Malik, 'COSAL—A black box compressible stability analysis code for transition prediction in three-dimensional boundary layers', *NASA CR-165925*, 1982.
20. M. R. Malik and D. I. Poll, 'Effect of curvature on three-dimensional boundary-layer stability', *AIAA J.*, **23,** 1362–1369 (1985).
21. C. M. Bender and S. A. Orszag, *Advanced Mathematical Methods for Scientists and Engineers*, McGraw-Hill, New York, 1978.